Stephen F. Austin State University

SFA ScholarWorks

Faculty Publications

Chemistry and Biochemistry

2003

Tetratricopeptide Repeat Motif-mediated Hsc70-mSTI1 Interaction MOLECULAR CHARACTERIZATION OF THE CRITICAL CONTACTS FOR SUCCESSFUL BINDING AND SPECIFICITY*

Odutayo O. Odunuge
Stephen F Austin State University, odunugaoo@sfasu.edu

Judith A. Hornby

Chrisiane Bies

Richard Zimmermann

David J. Pugh

See next page for additional authors

Follow this and additional works at: https://scholarworks.sfasu.edu/chemistry_facultypubs

Part of the Biochemistry Commons, and the Chemistry Commons

Tell us how this article helped you.

Authors

Odutayo O. Odunuge, Judith A. Hornby, Chrisiane Bies, Richard Zimmermann, David J. Pugh, and Gregory L. Blatch

Odutayo O. Odunuga, Judith A. Hornby, Christiane Bies, Richard Zimmermann, David J. Pugh and Gregory L. Blatch

Access the most updated version of this article at doi: 10.1074/jbc.M206867200

Find articles, minireviews, Reflections and Classics on similar topics on the JBC Affinity Sites.

Alerts:

- When this article is cited
- When a correction for this article is posted

Click here to choose from all of JBC's e-mail alerts

This article cites 32 references, 14 of which can be accessed free at
http://www.jbc.org/content/278/9/6896.full.html#ref-list-1

Tetratricopeptide Repeat Motif-mediated Hsc70-mSTI1 Interaction

MOLECULAR CHARACTERIZATION OF THE CRITICAL CONTACTS FOR SUCCESSFUL BINDING AND SPECIFICITY*

Odutayo O. Odunuga‡§, Judith A. Hornby‡, Christiane Bies¶, Richard Zimmermann¶, David J. Pugh∥, and Gregory L. Blatch‡**

From the ‡Department of Biochemistry, Microbiology and Biotechnology, Rhodes University, Grahamstown 6140, South Africa, ¶Medizinische Biochemie und Molekularbiologie, Universität des Saarlandes, D-66421 Homburg, Germany, and the ∥Department of Biotechnology, University of the Western Cape, Bellville 7535, Cape Town, South Africa

Murine stress-inducible protein 1 (mSTI) is a co-chaperone that is homologous with the human Hsp70/Hsp90-organizing protein (Hop). Guided by Hop structural data and sequence alignment analyses, we have used site-directed mutagenesis, co-precipitation assays, circular dichroism spectroscopy, steady-state fluorescence, and surface plasmon resonance spectroscopy to both qualitatively and quantitatively characterize the contacts necessary for the N-terminal tetratricopeptide repeat domain (TPR1) of mSTI1 to bind to heat shock cognate protein 70 (Hsc70) and to discriminate between Hsc70 and Hsp90. We have shown that substitutions in the first TPR motif of Lys^8 or Asn^{12} did not affect binding of mSTI1 to Hsc70, whereas double substitution of these residues abrogated binding. A substitution in the second TPR motif of Asn^{43} lowered but did not abrogate binding. Similarly, a deletion in the second TPR motif coupled with a substitution of Lys^8 or Asn^{12} reduced but did not abrogate binding. These results suggest that mSTI1-Hsc70 interaction requires a network of interactions not only between charged residues in the TPR1 domain of mSTI1 and the EEVD motif of Hsc70 but also outside the TPR domain. We propose that the electrostatic interactions in the first TPR motif made by Lys^8 or Asn^{12} define part of the minimum interactions required for successful mSTI1-Hsc70 interaction. Using a truncated derivative of mSTI1 incapable of binding to Hsp90, we substituted residues on TPR1 potentially involved in hydrophobic contacts with Hsc70. The modified protein had reduced binding to Hsc70 but now showed significant binding capacity for Hsp90. In contrast, topologically equivalent substitutions on a truncated derivative of mSTI1 incapable of binding to Hsc70 did not confer Hsc70 specificity on TPR2A. Our results suggest that binding of Hsc70 to TPR1 is more specific than binding of Hsp90 to TPR2A with serious implications for the mechanisms of mSTI1 interactions with Hsc70 and Hsp90 *in vivo.*

Hsp70/Hsp90-organizing protein (Hop)[1] (1, 2) and mSTI1 (3, 4) are homologous members of the stress-inducible protein 1 (STI1) family of co-chaperones. mSTI1 has 97% amino acid identity with Hop (4). Hop functions at an intermediate stage of the assembly of progesterone receptor by acting as an adaptor protein between Hsc70 and Hsp90 to form a multichaperone complex (2, 5). Both Hop and mSTI1 interact with Hsc70 and Hsp90 via their N-terminal and first central tetratricopeptide repeat domains, respectively (3, 6). The so-called tetratricopeptide repeat (TPR) motif is a degenerate 34-amino acid sequence that has been recruited by a significant number of co-chaperones that interact especially with Hsp90 (7–16). It is often found in multiple copies and in tandem array in proteins (17, 18). A typical TPR motif consists of two anti-parallel α helices with small consensus hydrophobic residues occurring at position of closest contact between the helices whereas large consensus residues are usually found at interfaces between adjacent helices in a tandem array (17–19). In multiple-motif TPR proteins, tandem TPR motifs fold into a right-handed superhelical structure forming a binding groove to accommodate partner proteins (19). Experimental evidence suggests that conserved basic residues that project into the grooves of the TPR domains of proteins that interact with Hsc70 and Hsp90 are important for binding to these molecular chaperones (20).

The crystal structures of the N-terminal TPR domain (TPR1) of Hop in complex with the C-terminal heptapeptide of Hsp70 and the first central TPR domain (TPR2A) in complex with the C-terminal pentapeptide of Hsp90 have been determined (6). The structures predict that binding involves a network of electrostatic interactions between charged amino acid residues in the N-terminal and first central TPR domains of Hop and the C-terminal EEVD motifs of Hsp70 and Hsp90 peptides, respectively. Recently, it has been shown that, whereas Asp^0 and Val^{-1} act as general anchor residues, the highly conserved glutamates of the EEVD motif, which appear to be critical in Hsp90 binding by TPR2A, do not contribute appreciably to the interaction of Hsp70 with TPR1 (21). The electrostatic interactions between the TPR domains and the C-terminal aspartate (Asp^0) form a two-carboxylate clamp that appears to be necessary for binding of Hop to Hsp70 and Hsp90. Residues in the TPR1 domain predicted to be involved in forming this clamp include Lys^8, Asn^{12}, Asn^{43}, Lys^{73}, and Arg^{77}, whereas the topologically equivalent residues in the TPR2A domain are Lys^{229}, Asn^{233}, Asn^{264}, Lys^{301}, and Arg^{305}. These amino acid

[1] The abbreviations used are: Hop, Hsp70/Hsp90-organizing protein; GST, glutathione *S*-transferase; TPR, tetratricopeptide repeat; PBS, phosphate-buffered saline; PMSF, phenylmethylsulfonyl fluoride; STI1, stress-inducible protein 1.

residues are highly conserved in TPR-containing proteins that bind to the C-terminal EEVD motifs of Hsc70 and Hsp90.

Discrimination between the C termini of the two molecular chaperones appears to depend largely on hydrophobic and van der Waals interactions between residues in the TPR domains of Hop and residues upstream of the EEVD motif (6, 21). For example, Ala[46], Ala[49], and Lys[50], all in helix A of the second TPR motif (helix 2A) in TPR1 of Hop, make hydrophobic contacts with the isoleucine (Ile^{-4}) of the IEEVD sequence in Hsp70, whereas Tyr[236] and Glu[271] in helix A of the first TPR motif (helix 1A) and helix A of the second TPR motif (helix 2A) of TPR2A, respectively, make important hydrophobic contacts with the methionine (Met^{-4}) of the MEEVD sequence in Hsp90. Pro^{-6}, which is further upstream of the EEVD motif in Hsp70, exists in a hydrophobic cavity formed by Glu[83] and Phe[84] of helix A of the third TPR motif (helix 3A) in TPR1. Val^{-1} in the EEVD motif of Hsp70 makes hydrophobic contacts with Asn[12] and Leu[15] in helix 1A and with Asn[43] in helix 2A of TPR1. In the TPR2A complex, Val^{-1} in the EEVD motif of Hsp90 is in hydrophobic contacts with Asn[233], Asn[264], and Ala[267].

The relevance of the individual amino acids in the C-terminal peptides of Hsp70 (PTIEEVD) and Hsp90 (MEEVD) to the Hsp70-Hop-Hsp90 complex, and in particular the Hsp90-Hop complex, has been characterized (21). However, the relative significance of the individual amino acids in the TPR1 domain groove to general binding and specificity of the Hsp70-Hop complex has yet to be experimentally characterized. Using site-directed mutagenesis, co-precipitation assays, circular dichroism spectroscopy, steady-state fluorescence, and surface plasmon resonance spectroscopy, we provide both qualitative and quantitative evidence to show that mSTI1-Hsc70 interaction requires a network of interactions not only between charged residues in the TPR1 domain of mSTI1 and the EEVD motif of Hsc70, but also outside the TPR domain. We also propose that the electrostatic interactions in the first TPR motif made by Lys[8] or Asn[12] define part of the minimum interactions required for successful mSTI1-Hsc70 interaction. Furthermore, we provide evidence that hydrophobic contacts in the second TPR motif of TPR1 domains are important in determining specificity of mSTI1 interaction with Hsc70, and by doing amino acid substitutions, we have engineered the ability to bind Hsp90 on the Hsc70-specific TPR1 domain of mSTI1. In contrast, engineering Hsc70-binding capacity on the Hsp90-binding TPR2A was not possible by simple swapping of topologically equivalent residues.

EXPERIMENTAL PROCEDURES

General Procedures—General molecular biology procedures such as restriction enzyme digestion, agarose gel electrophoresis, ligation, preparation of competent bacterial cells, and bacterial cell transformation were done according to standard protocols (22). Protein concentrations were determined using the Bradford protein assay (23). SDS-PAGE was performed according to Laemmli (24) and Western blotting according to Towbin *et al.* (25). The enhanced chemiluminescence system (ECL; Amersham Biosciences) was used to detect specific proteins during Western analysis.

Oligonucleotide-directed Mutagenesis—All mutations were generated from the plasmids pGEX3X2000 and pQE30–2000, which contain the cDNAs encoding the full-length proteins GST-543 and His-543, respectively. Generation of the deletion plasmids pGEX3X700 (encoding GST fusion of the C-terminal truncated protein, GST-N217), pGEX3X1400 (encoding GST fusion of the N-terminal truncated protein, GST-C334), and pGEX3X2000 (Δ37–47) (encoding GST fusion of the protein in which residues 37–47 have been deleted, GST-543 (Δ37–47)) has been previously reported (3, 26). All mutations were carried out by site-directed mutagenesis using a double-stranded whole plasmid linear amplification procedure (QuikChange mutagenesis kit; Stratagene, La Jolla, CA). Silent mutations were engineered to create restriction sites for screening purposes except where the desired codon

change(s) automatically generated restriction sites. The following alanine (Ala) mutant proteins were generated: GST-543 (K8A), GST-543 (N12A), GST-543 (K8A,N12A), His-543 (K8A,N12A), GST-543 (N43A), GST-543 (Δ37–47, K8A), GST-543 (Δ37–47, N12A), and GST-543 (K301A). GST-543 (Y27A) was generated as previously described (26). In the deletion mutant, a highly conserved block of amino acids in helix 2A (residues 37–47) was deleted. Other mutants generated are: GST-N217 (L15Y), GST-N217 (A49F,K50E), GST-N217 (L15Y,A49F,K50E), GST-C334 (Y236L), GST-C334 (F270A,E271K), and GST-C334 (Y236L,F270A,E271K). All mutations were confirmed both by restriction enzyme analysis and by DNA sequencing using the ABI PRISM 3100 Genetic Analyzer.

Production and Purification of GST-mSTI1 Fusion Proteins—Exponentially growing *Escherichia coli* XLI Blue cells carrying pGEX3X-derived plasmid constructs were induced for 5–6 h at 37 °C with 1 mM isopropyl-1-thio-β-D-galactopyranoside. The cells were harvested and lysed by mild sonication in 0.01 culture volume of ice-cold phosphate-buffered saline (PBS; 137 mM NaCl, 2.7 mM KCl, 4.3 mM Na$_2$HPO$_4$, 1.4 mM KH$_2$PO$_4$, pH 7.3) containing 1 mM final concentration of phenyl-methylsulfonyl fluoride (PMSF). The sonicate was incubated, with gentle agitation, for 30 min at room temperature after addition of Triton X-100 to 1% final concentration. The extracts were clarified by centrifugation at $12,000 \times g$ for 20 min at 4 °C. Aliquots of clarified extracts were added to 50% (w/v) slurry of glutathione-agarose beads (2-ml bed volume per 100 ml of extract) previously equilibrated with PBS. Binding was allowed to occur for 1 h at 4 °C with gentle rocking. After the beads were washed extensively with ice-cold PBS, the bound GST fusion proteins were eluted by adding appropriate volume of the elution buffer (10 mM reduced glutathione in 50 mM Tris-HCl, pH 8.0). Eluted GST fusion proteins were analyzed by 12% SDS-PAGE. Both wild-type and mutant proteins were expressed easily and found to be soluble.

Production and Purification of His$_6$-tagged mSTI1 Proteins—Heterologous production of His$_6$-tagged mSTI1 proteins in exponentially growing *E. coli* cells was induced by 1 mM isopropyl-1-thio-β-D-galacto-pyranoside. The *E. coli* cells were treated and lysed as described above. The clarified lysate was loaded onto a nickel-nitrilotriacetic acid resin column. Washing of the column was done using a buffer containing 50 mM Na$_2$HPO$_4$, pH 7.5, 20 mM imidazole, and 1 mM PMSF. The protein was eluted with a linear gradient of 20–300 mM imidazole. The ligand was removed from the protein by gel filtration in a Sephadex G-25 column. Buffer exchange was achieved by loading the purified protein onto a hydroxyapatite column previously equilibrated with 20 mM K$_2$HPO$_4$, pH 7.5, and eluting with a linear gradient of 20–300 mM K$_2$HPO$_4$. The homogeneity of the protein was assessed by SDS-PAGE (12%) and size exclusion-high performance liquid chromatography using a LKB model 2150.

Glutathione-Agarose Co-precipitation Assays—In separate 1-ml reactions, GST-mSTI1 fusion proteins were coupled to glutathione-agarose beads to a final concentration of 0.3 μM. Binding was allowed to occur for 1 h at 4 °C, after which unbound fusion protein was removed by washing three times in ice-cold PBS. Hsc70 binding assays were conducted by incubating the coupled agarose beads with 250 μg of NIH 3T3 crude extracts in a 1-ml reaction volume using ice-cold PBS. In Hsp90 binding assays, purified Hsp90 rather than extract proteins was added to a final concentration of 0.025 μM. After incubation for 2 h at 4 °C, the beads were collected and washed extensively in ice-cold PBS to remove nonspecifically bound extract proteins. The bound proteins were solubilized in 70 μl of SDS sample buffer and 30 μl analyzed on a 12% SDS-PAGE. After transferring onto nitrocellulose membrane, co-precipitation of Hsc70 or Hsp90 with the GST-mSTI1 fusion proteins was revealed by immunodetection and chemiluminescent autoradiography using the monoclonal primary antibodies H5147 and H9010 specific for Hsc70 and Hsp90, respectively.

Surface Plasmon Resonance Spectroscopy—Surface plasmon resonance spectroscopy was performed using a Biacore X apparatus. All experiments were performed at 25 °C in PBS containing 0.005% P20 surfactant (buffer A). Monoclonal goat anti-GST antibody was covalently attached to carboxymethlylated dextran on a sensor chip CM5 via amine coupling according to the protocol from the manufacturer (Biacore AB, Uppsala, Sweden). Approximately 700 response units of GST-mSTI1 fusion protein were bound to the immobilized antibody. Recombinant GST was immobilized on a separate reference flow cell. The chip was equilibrated with buffer A before passing solutions containing increasing concentrations of purified Hsc70 or Hsp90 over the bound proteins at a flow rate of 10 μl/min. For competition experiments, mixture of full-length Hsc70 and Hsp90 (8 and 5 μM final concentrations, respectively) was pre-incubated at 25 °C before passing it over the immobilized mSTI1 proteins. Background binding to GST was sub-

tracted from each signal to account for nonspecific binding to GST. Data were analyzed using the BIAevaluation software version 2.2.4.

Spectroscopic Measurements—Fluorescence emission spectra and other fluorescence measurements were made at 25 °C in 20 mM sodium phosphate, 1 mM EDTA, pH 7.5. The intrinsic fluorescence (excitation at 295 nm) of the lone tryptophan in mSTI1 was measured for 2 μM protein between 300 and 400 nm in a PerkinElmer fluorescence spectrophotometer (27). Circular dichroism measurements were made using 8 μM amounts of each protein sample in a Jasco J-710 spectropolarimeter. Ellipticity values were collected (average of 10 runs) in both the near-UV (350–250 nm) and far-UV (250–200 nm) regions.

NIH 3T3 Cell Culture and Preparation of Cell Lysates—NIH 3T3 mouse fibroblast cells were cultured in Dulbecco's modified Eagle's medium supplemented with 10% fetal calf serum and 1% penicillin (100 units/ml)/streptomycin (100 μg/ml) solution, at 37 °C and 10% CO_2 until they reached 80–100% confluence. The cells were harvested by trypsinization followed by three washes with PBS. The harvested cells were resuspended in appropriate volume of lysis buffer (50 mM Tris-HCl, 150 mM NaCl, 0.02% sodium azide, 100 μg/ml PMSF, 1 μg/ml aprotinin, and 1% Triton X-100) and incubated at 4 °C for 10 min to allow lysis to occur. The lysate was centrifuged at 12,000 $\times$ *g* for 30 min at 4 °C, and the supernatant used immediately.

RESULTS

Residues in TPR Domains of mSTI1 Required for Binding the EEVD Motif Are Highly Conserved in Homologous TPR Domains—Fig. 1*A* shows the various GST-mSTI1 protein derivatives used in this study. For both steady-state and circular dichroism spectroscopies, we used the His$_6$-tagged proteins. We constructed a sequence alignment of Hsc70-interacting TPR domains of STI1 homologues. The alignment revealed that the charged residues in the TPR domains predicted to form the so-called two-carboxylate clamp with the EEVD motif of Hsc70 are strictly conserved among homologous STI1 proteins (Fig. 1*B*, *first alignment*). In another alignment, we compared the same basic residues in Hsc70-binding TPR domains of non-homologous Hsc70-interacting proteins of colon cancer antigen 7 (NY-CO-7; Ref. 28), C terminus of Hsc70-interacting protein (CHIP; Ref. 29), Hop (1), mSTI1 (4), human small glutamine-rich protein (hSGT; Ref. 28), tetratricopeptide repeat domain 1 (TPR1; Ref. 28), tetratricopeptide repeat domain 2 (TPR2; Ref. 28), and Hsc70-interacting protein (Hip; Ref. 30). Conservation was found to be less strict in these proteins, especially at positions equivalent to Lys[73] and Arg[77] in Hop (Fig. 1*B*, *second alignment*). As expected, the residues that are predicted to determine specificity of binding to Hsc70 in Hop do not show strict conservation when comparing functionally equivalent Hsc70-interacting TPR domains (Fig. 1*B*, *first* and *second alignments*). When comparing TPR1, TPR2A, and TPR2B domains of mSTI1, Ala[49] and Lys[50] in TPR1 are predicted to be topologically equivalent to Phe[270] and Glu[271] in TPR2A, and Thr[405] and Lys[406] in TPR2B, respectively (Fig. 1*B*, *third alignment*). Ala[49] and Lys[50] in Hop are predicted to be important in determining Hsc70 binding specificity, whereas Phe[270] and Glu[271] are predicted to be critical for the specific binding of Hsp90 (6). Interestingly, TPR2B has similar specificity determinants at these positions to those of TPR1 (Ala[49]/Lys[50] *versus* Thr[405]/Lys[406]), suggesting that it may have, yet to be detected, Hsc70-interaction capacity (Fig. 1*B*, *third alignment*). Fig. 2 (*A* and *B*) shows the ribbon representations of the crystal structures of the N- and C-terminal TPR domains of Hop in complex with the C-terminal peptides of Hsp70 and Hsp90, respectively. Amino acid residues involved in general binding (Fig. 2*A*, *i* and *ii*) and specificity of binding (Fig. 2*B*, *i* and *ii*) of the TPR domains to the peptides are represented in *sticks*. Homology modeling, using co-ordinates generated from Hop, revealed that the structures of the N- and C-terminal TPR domains of mSTI1 are similar to that of Hop. This is not unexpected because the two homologues share 97% amino acid identity.

Double Substitution of Lys[8] and Asn[12] in Helix A of the First TPR Motif of mSTI1 Abrogated Specific Binding to Hsc70—We performed charged-to-alanine scanning mutagenesis of some of the residues in mSTI1 that are predicted to be involved in forming the so-called two-carboxylate clamp with the EEVD sequence in Hsc70 and Hsp90. We generated single mutations: GST-543 (K8A), GST-543 (N12A), GST-543 (N43A), GST-543 (K301A), and a double mutation, GST-543 (K8A,N12A), of the full-length GST fusion protein (GST-543); and single mutations GST-543 (Δ37–47, K8A) and GST-543 (Δ37–47, N12A) of the deletion mutant GST-543 (Δ37–47) (see "Experimental Procedures"). GST-543 (K73A), GST-543 (R77A), GST-543 (K229A), and GST-543 (N233A) could not be produced successfully, possibly because of deleterious structural effects of the amino acid substitutions on the protein. The various GST fusion proteins were tested for their ability to bind to either Hsc70 from NIH 3T3 mouse fibroblast cell extracts or purified Hsp90. Our results showed that single mutation of Lys[8] or Asn[12] in helix 1A of TPR1 had no significant effect on the specific binding of mSTI1 to Hsc70, as these mutant proteins bound Hsc70 at levels comparable with that of the unmodified protein (Fig. 3*A*, *lanes 1*, *3*, and *5*). However, double mutation of Lys[8] and Asn[12], GST-543 (K8A,N12A), abrogated binding to Hsc70 below detectable levels (Fig. 3*A*, *lane 4*). In contrast to Hsc70-mSTI1 interaction, single substitution of Lys[301] in TPR2A, GST-543 (K301A), was found to abrogate binding of mSTI1 to Hsp90 (results not shown). Notably, mutation of Asn[43] in helix 2A of TPR1 led to a significant decrease in the affinity of mSTI1 for Hsc70 but not abrogation (Fig. 3*A*, *lane 7*). As a negative control (Fig. 3*A*, *lane 6*), we used a mutant GST derivative of mSTI1, GST-543 (Y27A), which has been shown not to bind Hsc70 (26). In all the binding assays, GST alone did not bind to Hsc70 (Fig. 3).

To provide evidence that binding of Hsc70 to the GST-mSTI1 derivatives was specific and not the recognition of misfolded proteins by Hsc70, we tested the sensitivities of the interactions to increasing ionic strength. The interaction of GST-543 appeared to be specific as binding of the unmodified protein was found to decrease with increasing ionic concentrations (result not shown). The binding of GST-543 (K8A), GST-543 (N12A), and GST-543 (N43A) followed the same pattern at increasing ionic concentrations (results not shown). Single alanine substitution of Lys[8] coupled with the deletion of a highly conserved block in helix 2A of TPR1, GST-543 (Δ37–47, K8A), significantly lowered but did not abrogate binding of mSTI1 to Hsc70 (Fig. 3*B*, *lane 5*). Similar result was obtained for the GST-543 (Δ37–47, N12A) mutant (result not shown). These latter results corroborate earlier reports from our laboratory (26). Taken together, these results showed that double substitution of Lys[8] and Asn[12] by alanine was required to abrogate binding of mSTI1 to Hsc70, whereas single substitution of Lys[301] was sufficient to abrogate its binding to Hsp90.

Hsp90-binding Capacity Was Engineered on the Hsc70-binding TPR1 Domain of mSTI1—Based on the predictions from the three-dimensional structure of the TPR domains of Hop in complex with their respective peptides (6), we identified those topologically equivalent residues involved in specificity determination that differed greatly, in TPR1 *versus* TPR2A, in the nature of their contacts with residues upstream of the EEVD motif of their respective Hsps. We observed that Tyr[236], Phe[270], and Glu[271] in TPR2A are significantly different from but topologically equivalent to Leu[15], Ala[49], and Lys[50] respectively, in TPR1 (Fig. 2*B*). We reasoned that by doing simple amino acid substitutions of L15Y, A49F, and K50E, and Y236L, F270A, and E271K, we could swap the binding specificity of TPR1 and TPR2A domains, respectively. Theoretically, these substitu-
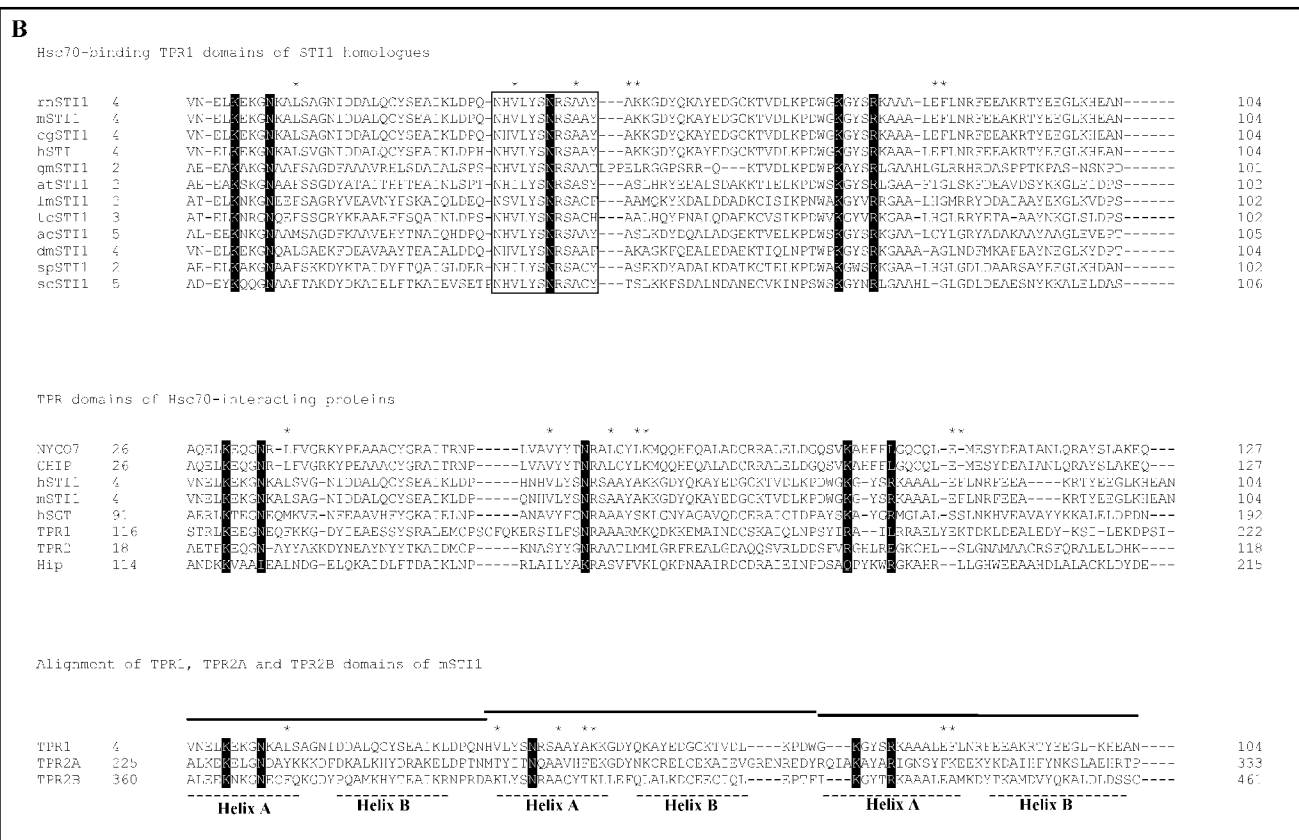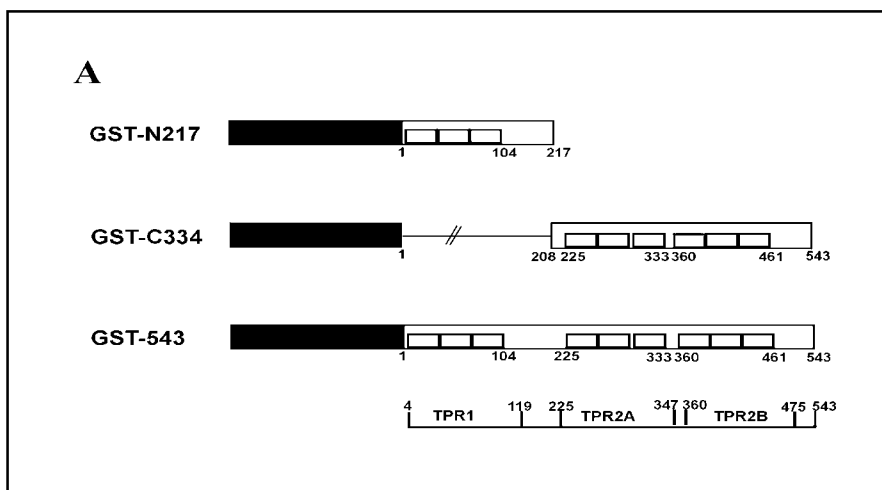
FIG. 1. **TPR domain organization in mSTI1 and multiple sequence alignment of TPR domains from Hsc70-interacting proteins.** *A*, schematic representation of GST-mSTI1 derivatives showing the GST tag (*large solid bars*), mSTI1 sequence (*large open bars*), TPR motifs (*small open bars*), and TPR domains (as indicated on grid). The *numbering* refers to amino acid positions in mSTI1. *B*, multiple sequence alignment of Hsc70-interacting TPR domains of STI1. Helices A and B of each TPR motif are shown beneath the alignment (*dashed lines*), whereas the complete TPR motifs are represented as *horizontal bars*. Residues that are predicted to form a two-carboxylate clamp with the terminal aspartate in Hsc70 are highlighted in *black*, whereas *asterisk* (*) indicates positions of residues predicted to determine specificity of binding. A highly conserved block of residues in the second TPR motif is shown in *unfilled box*. Hsc70-binding TPR1 domains of STI1 homologues: *rn* (*Rattus norvegicus*, CAA75351.1), *m* (*Mus musculus*, AAC53267.1), *cg* (*Cricetulus griseus*, AAB94760.1), *h* (*Homo sapiens*, AAA58682.1), *tc* (*Trypanosoma cruzi*, AAC97378.1), *ac* (*Achantamoeba castellanii*, AAB49720), *at* (*Arabidopsis thaliana*, CAB45987.1), *gm* (*Glycine max*, S56658), *dm* (*Drosophila melanogaster*, AAC12945.1), *lm* (*Leishmania major*, AAB37318), *sp* (*Schizosaccharomyces pombe*, CAB39910.1), *sc* (*Saccharomyces cerevisiae*, CAA60743.1). TPR1 domains of Hsc70-interacting proteins: NY-CO-7 (colon cancer antigen 7, AAC18038), CHIP (C terminus of Hsc70-interacting protein, AAK61242), hSTI1 (human STI1 or Hop, AAA58682.1), mSTI1 (murine STI1 or extendin, AAC53267.1), hSGT (human small glutamine-rich protein, NP_003012), TPR1 (tetratricopeptide repeat domain 1, NP_003305), TPR2 (tetratricopeptide repeat domain 2, NP_003306), and Hip (Hsc70-interacting protein, P50502). Alignment of TPR1, TPR2A, and TPR2B domains of mSTI1 was as follows: TPR1, N-terminal TPR domain of mSTI1; TPR2A, first central TPR domain of mSTI1; and TPR2B, second central TPR domain of mSTI1.

tions should allow TPR1 to accommodate Met^{-4} of Hsp90 and TPR2A to accommodate Ile^{-4} of Hsc70, respectively. We therefore proposed, first, that L15Y, A49F, and K50E substitutions in TPR1 domain of mSTI1 would result in loss of ability to bind

Hsc70 and gain of capacity to bind Hsp90, and second, that Y236L, F270A, and E271K substitutions in TPR2A would result in loss of ability to bind Hsp90 and gain of capacity to bind Hsc70. In the first part of our hypothesis, we generated single,
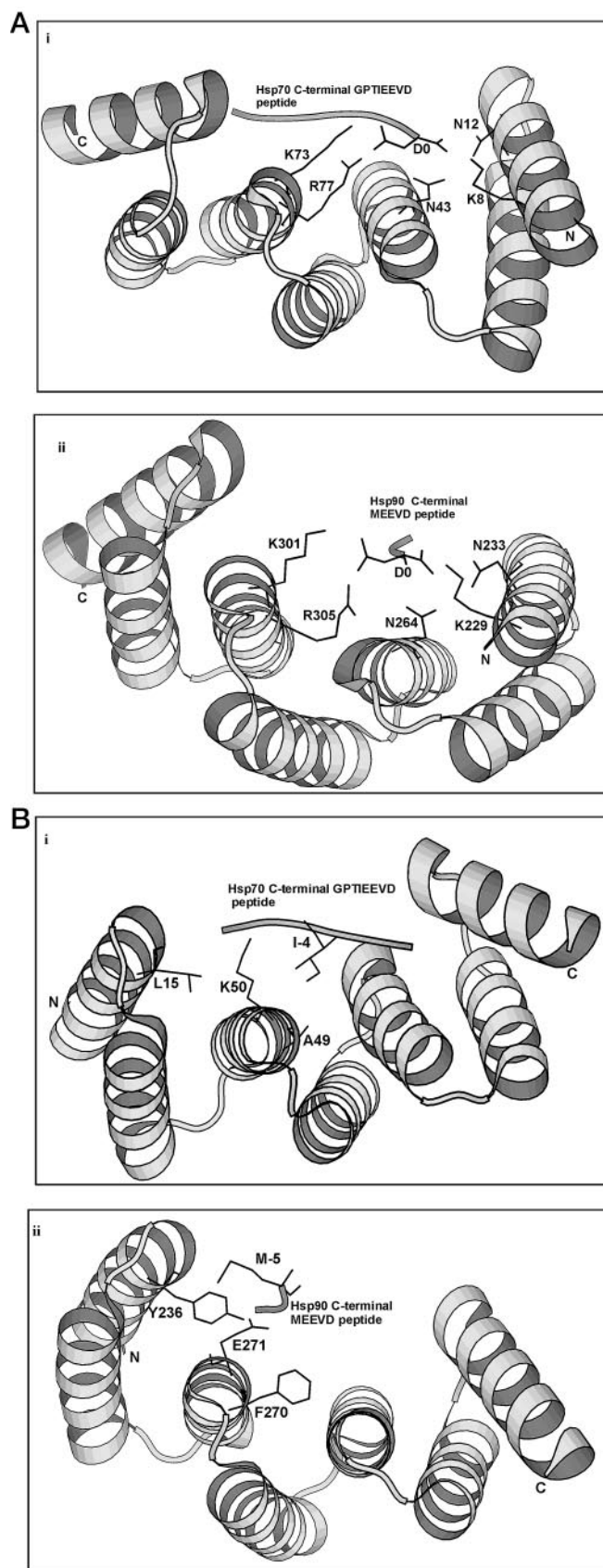
FIG. 2. **Hop TPR domains in complexes with C-terminal Hsc70 and Hsp90 peptides.** Ribbon representations of the crystal structures of the N-terminal TPR (TPR1; Protein Data Bank code 1ELW) and central TPR (TPR2A; Protein Data Bank code 1ELR) domains of Hop in complexes with the C-terminal heptapeptide of Hsp70 and pentapeptide of Hsp90, respectively. TPR domains are shown as *ribbons*, peptides as *rods*, and amino acid residues as *sticks*. The TPR residues are
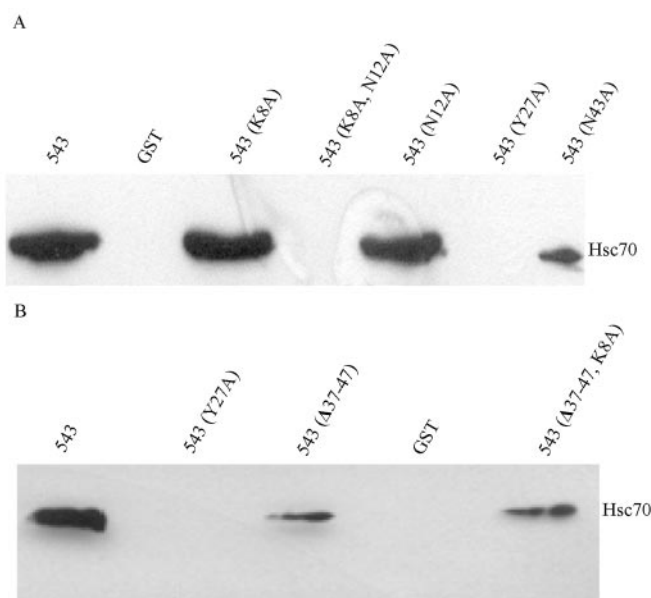

FIG. 3. **Hsc70-mSTI1 interaction is differentially perturbed by substitution of residues in mSTI1 predicted to be important for binding to Hsc70.** GST-mSTI1 fusion proteins (0.3 μM) previously coupled to glutathione-agarose beads were incubated with 250 μg of extracts of NIH 3T3 mouse fibroblasts for 2 h at 4 °C. The beads were washed extensively to remove unbound proteins. Bound proteins were solubilized in SDS sample buffer and separated by 12% SDS-PAGE. After transferring onto nitrocellulose membrane, co-precipitation of Hsc70 with the GST-mSTI1 fusion proteins was revealed by immuno-detection and chemiluminescent autoradiography. 543 is equivalent to GST-543 as described under "Experimental Procedures." Information in *brackets* indicates mutations carried out in the proteins.

double, and triple mutants using the C-terminal truncated mutant protein GST-N217 (TPR2A and TPR2B domains removed) as follows: GST-N217 (L15Y), GST-N217 (A49F,K50E), and GST-N217 (L15Y,A49F,K50E). These modified proteins were tested for their ability to bind both Hsc70 and Hsp90. In the Hsc70 co-precipitation assays, GST-N217 was found to associate with Hsc70 at levels that compared favorably with the full-length protein, GST-543 (Fig. 4*A*, *lanes 1* and *3*). As expected, both GST-543 (Y27A) and GST did not bind to Hsc70 (Fig. 4*A*, *lanes 2* and *4*). The single mutant GST-N217 (L15Y) bound to Hsc70 at a slightly lower level compared with GST-N217, whereas binding was significantly lowered using the double mutant GST-N217 (A49F,K50E) (Fig. 4*A*, *lanes 5* and *6*). No binding to Hsc70 was observed in the triple mutant GST-N217 (L15Y,A49F,K50E) (Fig. 4*A*, *lane 7*). We thus concluded that double substitution of Ala[49] and Lys[50] in mSTI1 drastically reduced binding to Hsc70, whereas triple substitution of Leu[15], Ala[49], and Lys[50] abolished binding. The next step was to test whether these mutants could interact with Hsp90. In this experiment, we used purified Hsp90 instead of cell lysates. As expected, both full-length unmodified protein GST-543 and N-terminal truncated protein GST-C334 (TPR1 domain deleted) bound to purified Hsp90 at equivalent levels (Fig. 4*B*, *lanes 1* and *3*). Additionally, the C-terminal truncated protein GST-N217, its mutant derivative GST-N217 (L15Y) and GST alone did not bind to Hsp90 as expected (Fig. 4*B*,

labeled by the *single-letter code* and a *number* that relates to its position in the primary amino acid sequence. *A*, basic residues in TPR domains of Hop form a network of electrostatic interactions with terminal aspartate (Asp[0]) in Hsp70 (*i*). Hsp90 binds to the central TPR domain (TPR2A) of Hop by a similar mechanism (*ii*). *B*, specificity of binding is determined by hydrophobic contacts with Ile[−4] in Hsp70 (*i*) and Met[−5] in Hsp90 (*ii*). The panels were drawn using MOLSCRIPT (32).

A

B
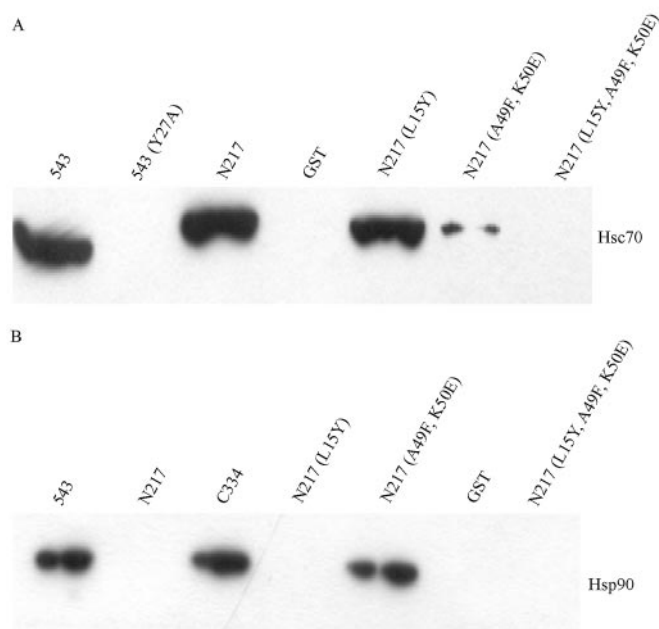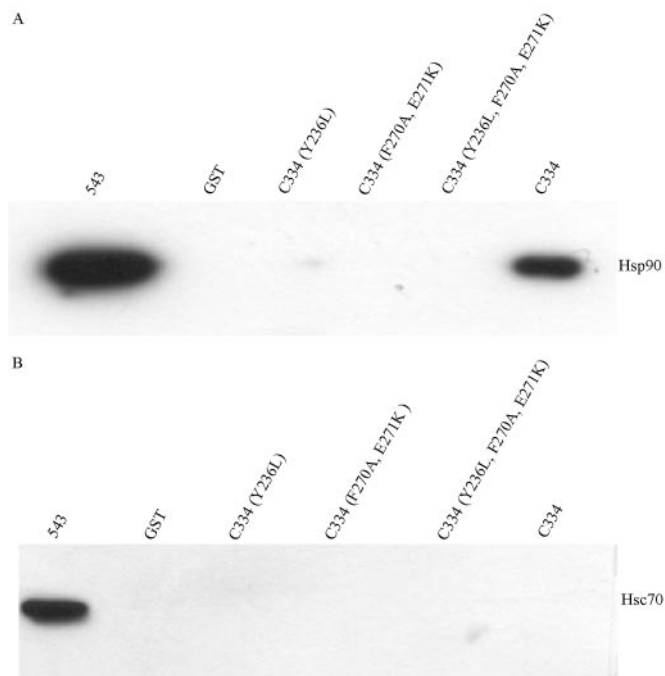

FIG. 4. **Hsp90-binding capacity was engineered on the Hsc70-binding TPR1 domain of mSTI1.** GST-mSTI1 fusion proteins (0.3 μM) previously coupled to glutathione-agarose beads were incubated with 250 μg of extracts of NIH 3T3 mouse fibroblasts (*A*) or purified Hsp90 (0.025 μM; *B*) for 2 h at 4 °C. Further steps were the same as described in Fig. 3. 543 is equivalent to GST-543, N217 to GST-N217, and C334 to GST-C334 as described under "Experimental Procedures." Information in *brackets* indicates mutations carried out in the proteins.

A

B

FIG. 5. **Hsc70-binding capacity could not be engineered onto the Hsp90-binding TPR2A of mSTI1.** GST-mSTI1 fusion proteins (0.3 μM) previously coupled to glutathione-agarose beads were incubated with purified Hsp90 (0.025 μM; *A*) or 250 μg of extracts of NIH 3T3 mouse fibroblasts (*B*) for 2 h at 4 °C. Further steps were the same as described in Fig. 3. 543 is equivalent to GST-543 and C334 to GST-C334 as described under "Experimental Procedures." Information in *brackets* indicates mutations carried out in the proteins.

lanes 2, *4*, and *6*). Interestingly, the double mutant GST-N217 (A49F,K50E) was found to bind to Hsp90 at levels comparable with both GST-543 and GST-C334 (Fig. 4*B*, *lane 5*). Surprisingly, no Hsp90 binding was observed with the triple mutant GST-N217 (L15Y,A49F,K50E) (Fig. 4*B*, *lane 7*). Put together, these results suggested that double mutation of Ala[49] and Lys[50] by Phe and Glu, respectively, was sufficient to confer the ability to bind Hsp90 on the Hsc70-binding TPR1 domain of mSTI1.

Hsc70-binding Capacity Could Not Be Engineered onto the TPR2A Domain—We used the N-terminal truncated mutant protein GST-C334, incapable of binding to Hsc70, to generate the following modified proteins: GST-C334 (Y236L), GST-C334 (F270A,E271K), and GST-C334 (Y236L,F270A,E271K) and tested them for their ability to bind to both Hsp90 and Hsc70. Both GST-543 and GST-C334 were found to bind Hsp90 as expected (Fig. 5*A*, *lanes 1* and *6*). GST did not bind to Hsp90 (Fig. 5*A*, *lane 2*). Interestingly, the single, double, and triple mutant proteins, GST-C334 (Y236L), GST-C334 (F270A,E271K), and GST-C334 (Y236L,F270A,E271K), respectively, lost their ability to bind to Hsp90 (Fig. 5*A*, *lanes 3*, *4*, and *5*). Next, the proteins were tested for their ability to bind to Hsc70. GST-543 was found to bind to Hsc70 successfully, whereas GST did not (Fig. 5*B*, *lanes 1* and *2*). None of the GST-C334 mutants were able to bind to Hsc70 (Fig. 5*B*, *lanes 3*, *4*, and *5*). These results indicated that single mutation of any of the residues in TPR2A that make hydrophobic contacts with the C-terminal peptide of Hsp90 abrogated binding of mSTI1 to Hsp90. In addition, engineering Hsc70-binding capacity on TPR2A was not possible by simple swapping of topologically equivalent residues.

Hsc70 Potentially Makes Contact with mSTI1 outside the N-terminal TPR Domain—Steady-state fluorescence and circular dichroism spectroscopies were used to analyze the effects of mutations on both the secondary (far- and near-UV) and tertiary structures (steady-state fluorescence) of the His$_6$-tagged mSTI1 proteins. The intrinsic fluorescence of the lone trypto-

phan in mSTI1 (Trp[71]) was monitored. This tryptophan is located in helix B of the second TPR motif, a position in relatively close proximity to the regions of the mutations, and therefore could serve effectively as a local probe. Notable results were obtained with the His$_6$-tagged double mutant, His-543 (K8A,N12A). The fluorescence profile of the wild type protein (His-543) showed a characteristic peak at 345 nm (Fig. 6*A*), indicative of a partially buried residue. Completely exposed residues give a wavelength peak in the vicinity of 357 nm. The fluorescence profile of the His-543 (K8A,N12A) mutant revealed an identical peak wavelength at 345 nm with a slight increase in intensity. This indicated a similar environment surrounding the tryptophan residue in both proteins and suggested that there was no significant change in the tertiary structure of the TPR1 domain resulting from the mutations. Interestingly however, both far- and near-UV circular dichroisms revealed an apparent loss of helical content in the His-543 (K8A,N12A) variant protein. This was illustrated by the decrease in ellipticity observed in the spectra of the double mutant protein (Fig. 6*B*). Together, these results suggested that the apparent loss of helical content might have occurred in other parts of the protein that interact with the N-terminal TPR domain and make contact with Hsc70 upon binding.

Quantitative Analysis of mSTI1-Hsc70 Interactions—To determine the contribution of each individual amino acid residue to the binding of Hsc70 by mSTI1, we used surface plasmon resonance spectroscopy to monitor bimolecular interactions. Unmodified mSTI1 and its mutants were immobilized on biosensor chip equilibrated with buffer A. GST was bound to a reference flow cell and used as a control. Subsequently, increasing concentrations of full-length Hsc70 and Hsp90 were then passed over the chip and binding of the proteins was monitored (Figs. 7 and 8). Thermodynamic dissociation constants (K_D values) were determined and taken as apparent affinities of
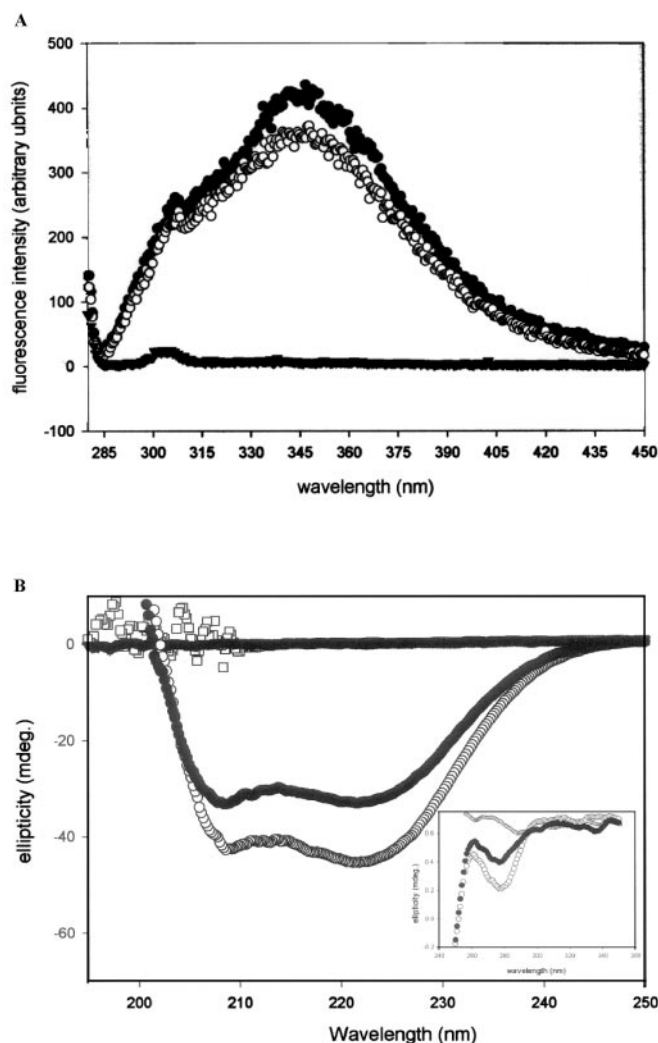
FIG. 6. **Double substitution of Lys[8] and Asn[12] in mSTI1 potentially perturbed contacts made outside the TPR1 domain.** *A*, steady-state fluorescence using the lone tryptophan (Trp[71]) in His-543 (*open circles*) and His-543 (K8A,N12A) (*closed circles*). Excitation was done at 295 nm wavelength. *B*, far-UV circular dichroism spectra of His-543 (*open circles*) and His-543 (K8A,N12A) (*closed circles*) in 20 mM sodium phosphate buffer, pH 7.5. Spectra are an average of 10 runs. The *inset* describes the near-UV dichroism spectra of His-543 (*open circles*) and His-543 (K8A,N12A) (*closed circles*) in the same buffer.

FIG. 7. **Binding affinities of mSTI1 and its mutants to Hsc70.** *A*, Hsc70 was titrated against GST-543 using surface plasmon resonance spectroscopy to determine binding affinity. Experiments were performed at 25 °C in PBS containing 0.005% P20 surfactant. Approximately 700 response units of GST-543 fusion protein were immobilized on a sensor chip CM5 on which anti-GST was previously attached via amine coupling to carboxymethylated dextran. Increasing concentrations of Hsc70 were injected at a flow rate of 10 μl/min. Recombinant GST was immobilized on a reference flow cell, and background binding to GST was subtracted from each signal. *B*, relative binding response curves of GST-543 and its mutants to Hsc70 (8 μM).

binding. However, it should be noted that the kinetics of binding could not be fitted perfectly to a 1:1 Langmuir binding model. The K_D of the binding of unmodified mSTI1 protein to Hsc70 was calculated to be ~2 μM (Fig. 7*A*). Generally, the K_D values of the mutant mSTI1 proteins were significantly higher than that of the unmodified mSTI1, indicating reduced binding affinities (Fig. 7*B*). It is notable that most of the mutants displayed predominantly rapid kinetics (Fig. 7*B*). In the Hsp90 binding assays, the unmodified mSTI1 (543; Fig. 8) displayed kinetics similar to its interaction with Hsc70 and the K_D was calculated to be 1.5 μM. These K_D values are similar to earlier reports (21). A very interesting observation was the higher affinity of the N217 (A49F,K50E) mutant protein, K_D of 0.15 μM, compared with the wild type protein. Interestingly, even in the presence of Hsc70, the protein was still able to bind to Hsp90 to the same affinity (Fig. 8*B*). From these results we can conclude that mutation of any of the residues in TPR1 of mSTI1 that form the so-called two-carboxylate clamp reduces its affinity to bind to Hsc70 and that the individual amino acid residues contribute differentially to the network of electrostatic contacts.
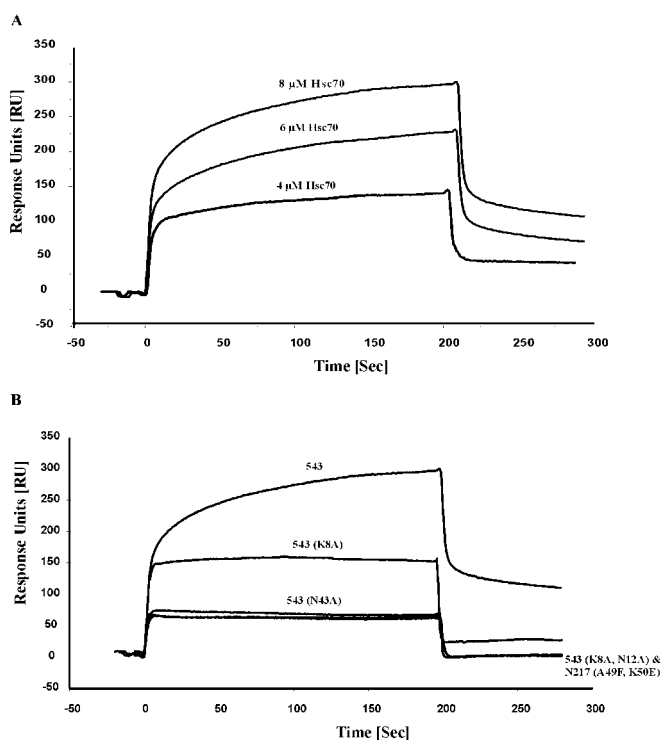
DISCUSSION

Based on mutational analyses, the Hsc70 and Hsp90 interacting domains of Hop and mSTI1 have been mapped to their N- and C-terminal TPR domains, respectively (3, 5, 6, 26). We have shown that the amino acid residues 1–109 in the N-terminal TPR domain in mSTI1, without extensive flanking regions, are necessary and sufficient for its interaction with Hsc70 (26). In addition, our results suggested that the consensus residue Tyr[27] in the first TPR motif of mSTI1 might play a crucial structural role by holding charged residues in the first TPR motif in position for interaction with complementary charged groups of Hsc70. The crystal structure of the TPR1 domain of Hop in complex with C-terminal Hsp70 heptapeptide predicts that certain basic residues protruding into the TPR groove are required for its interaction with Hsp70 (6). Furthermore, the structure suggests that hydrophobic contacts are critical in determining specificity of binding of Hop to Hsp70. We have further characterized these interactions both qualitatively and quantitatively, in an mSTI1-Hsc70 model.

Among the residues in Hop predicted to be required for formation of a critical two-carboxylate clamp with the C-terminal aspartate (Asp[0]) of the Hsp70 peptide are Lys[8], Asn[12], Asn[43], Lys[73], and Arg[77] (6). Multiple sequence alignments (Fig. 1*B*) revealed that Lys[8], Asn[12], and Asn[43] are strictly conserved in Hsc70-interacting TPR motifs including those from non-homologous proteins. Except for Hip, all these proteins interact with Hsc70 via its C-terminal EEVD motif (28). The side chains of Lys[8] and Asn[12] were proposed to form direct hydrogen bonds with the C-terminal main-chain carboxylate of Asp[0] in Hsp70 (6). Although co-precipitation assays indicated that mutation of
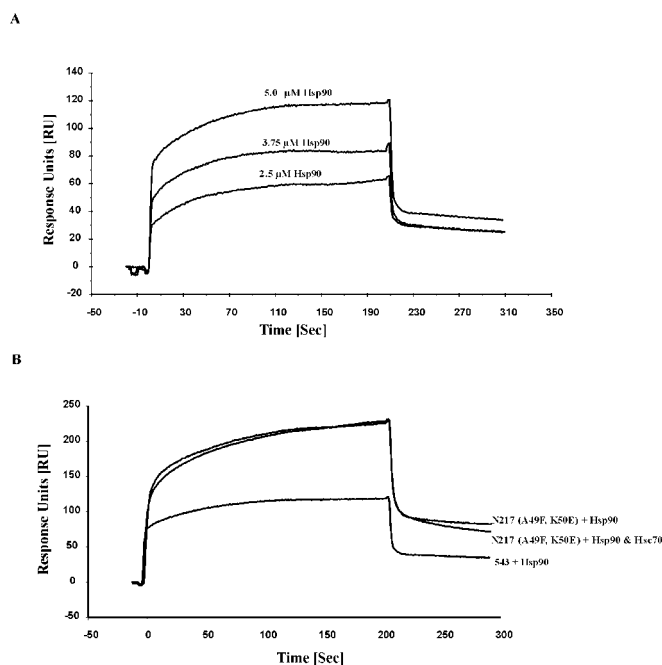
FIG. 8. **Binding affinities of mSTI1 and its mutants to Hsp90.** *A*, Hsp90 was titrated against GST-543 using surface plasmon resonance spectroscopy to determine binding affinity. Experiments were performed as described in Fig. 7. *B*, relative binding response curves of GST-543 and its mutants to Hsp90 (5 μM).

these residues singly to alanine did not significantly affect binding of mSTI1 to Hsc70, surface plasmon resonance spectroscopy revealed a significant reduction in the binding affinities of the mutant proteins to Hsc70. The SPR results may be regarded as being more reliable because the technique is both quantitative and highly sensitive compared with co-precipitation assays. However, both assays revealed that double mutation of these residues to alanine abrogated binding of mSTI1 to Hsc70. In addition to these, results from steady-state fluorescence and circular dichroism spectroscopies strongly suggested that these mutations in mSTI1 might have caused perturbations in parts of the protein outside the TPR1 domain, resulting in loss of helical content. Hence, the observed abrogation of binding to Hsc70 might have occurred primarily as a result of loss of important electrostatic contacts with the TPR domain and secondarily as a result of disruption of contacts with other domains required for complete interaction with Hsc70. Support for this hypothesis comes from earlier observation that mutation of the C-terminal DPEV motif of Hop or its DPAM to APAV and APAM, respectively, caused a reduction in the ability of Hop to bind to Hsp70 (31). This is a very interesting phenomenon because truncation of this region from Hop caused only a partial loss in Hsp70 binding (5). In a helix-rich protein such as mSTI1, it is most likely that this C-terminal region of the protein folds into a helical structure. Of interest, however, is the observation that binding of Hop to Hsp90 was unaffected by mutations in this region (31). Therefore, we conclude that the collective electrostatic contacts made by Lys[8] and Asn[12] in TPR1 domain of mSTI1 define part of the minimum critical contacts necessary for successful binding to Hsc70 but for complete and tight ligand binding other contacts outside the TPR domain are required.

Mutation of Asn[43] to alanine significantly lowered but did not abrogate mSTI1-Hsc70 interaction. Asn[43] occurs within helix A of the second TPR motif (helix 2A), a region that is highly conserved in homologous STI1 TPR domains. Deletion of this highly conserved block of amino acid residues coupled with

the mutation of Lys[8] or Asn[12] alone to alanine significantly lowered but did not abrogate binding of mSTI1 to Hsc70. This result is consistent with and extends our earlier report that removal of the highly conserved part of helix 2A lowered but did not abolish binding of mSTI1 to Hsc70 (26). It is possible that there is a shifting of the helices to compensate for the loss of helix 2A. The side-chain carbonyl of Asn[43] makes a direct hydrogen bond contact with the backbone amide of Asp[0] of Hsc70, and an indirect contact with the side-chain carboxylate of the same residue that is mediated by a tightly bound water molecule. The interactions of Asn[43] and other helix 2A residues appear not to be as important for Hsc70 binding as the electrostatic contacts made collectively by Lys[8] and Asn[12] with Asp[0]. Our results, which are partially consistent with crystallographic predictions for the Hop-Hsp70 peptide complex, suggested that a network of electrostatic interactions was necessary for the binding of mSTI1 to Hsc70. In addition, our results suggested that electrostatic interactions involving residues in the first TPR motif (Lys[8] and Asn[12]) might be more critical for successful mSTI1-Hsc70 interaction than those electrostatic interactions involving residues in the second TPR motif (Asn[43]). Interestingly, however, single substitution of Lys[301] in the central TPR domain of mSTI1 caused an abrogation of its interaction with Hsp90. We can infer from these observations that, even though the mechanisms of binding of TPR1 and TPR2A domains of mSTI1 or Hop to their respective peptides look similar, they are not exactly identical.

The crystal structures of the Hop TPR domains in complex with Hsp70 and Hsp90 peptides predict that certain residues in Hop make hydrophobic and van der Waals contacts with residues in the peptides, and that these interactions discriminate between the C termini of Hsp70 and Hsp90. Based on these data and sequence alignments, we hypothesized that by doing L15Y, A49F, and K50E substitutions, we could engineer TPR1 to accommodate the Met[−4] upstream of the Hsp90 C-terminal EEVD motif and hence bind Hsp90 with high affinity. Conversely, by doing Y236L, F270A, and E271K substitutions in TPR2A, we hypothesized that we could engineer this domain to bind to Hsc70. For the first hypothesis, we used a C-terminal truncated GST fusion derivative of mSTI1, GST-N217, that lacks the Hsp90-binding TPR domain. As expected, the L15Y substitution alone only slightly lowered the affinity of mSTI1 for Hsc70. However, GST-N217 (L15Y) did not bind to Hsp90. This observation may be the result of the fact that substituting Tyr for Leu did not provide enough hydrophobic contacts for the mutant mSTI1 to interact successfully with Hsp90. Interestingly, the double mutant GST-N217 (A49F,K50E) bound to Hsc70 with low affinity, whereas it successfully bound to Hsp90 with an affinity even higher than that of the full-length unmodified protein, as indicated by SPR spectroscopy. Therefore, substitution of Ala[49] and Lys[50] to Phe and Glu, respectively, in mSTI1 resulted in drastic loss of ability to bind Hsc70 but gain of ability to bind Hsp90 with high affinity. Surprisingly, the triple mutant GST-N217 (L15Y,A49F,K50E) lost ability to bind to both Hsc70 and Hsp90. Although Leu[15] may be involved in specificity, its proximity to Lys[8] and Asn[12] may suggest that any changes in this region will disturb the two-carboxylate clamp sufficiently to cause the triple mutant GST-N217 (L15Y,A49F,K50E) to lose its capacity to bind to Hsp90. For the second hypothesis, we used an N-terminal truncated GST fusion derivative of mSTI1 (GST-C334), which lacks the Hsc70-binding TPR domain. All three modified proteins, GST-C334 (Y236L), GST-C334 (F270A,E271K), and GST-C334 (Y236L,F270A,E271K), could not bind to either Hsc70 or Hsp90. These results suggest that binding of Hsc70 to mSTI1 or Hop is more specific than the binding of Hsp90 with serious

implications for the sequential interaction of mSTI1 or Hop to Hsc70 and Hsp90 *in vivo*. It has been reported recently that the affinity of Hsp70 for Hop increases in the presence of Hsp90 and that Hsp90 reduces the number of Hsp70 binding sites on the Hop dimer (33).

In conclusion, first, we have provided evidence to show that hydrophobic contacts in the second TPR motif (Ala[49] and Lys[50]) of TPR1 may be more important than other regions of this domain in determining specificity of mSTI1 interaction with Hsc70. Second, we have successfully engineered Hsp90 binding capacity on the TPR1 domain of mSTI1 by doing simple amino acid substitutions without elaborate "domain swapping." Third, we have shown that the mechanisms of interaction of mSTI1 with Hsc70 and Hsp90 are not identical. Although our data further the understanding of the molecular basis of the interaction of mSTI1/Hop with Hsc70 and Hsp90, more mutagenesis studies and the three-dimensional structures of mSTI1/Hop in complex with full-length Hsc70 and Hsp90 are needed for a more complete understanding of the mechanisms of interaction.

REFERENCES

1. Honore, B., Leffers, H., Madsen, P., Rasmussen, H. H., Vandekerckhove, J., and Celis, J. E. (1992) *J. Biol. Chem.* **267,** 8485–8491
2. Smith, D. F., Sullivan, W. P., Marion, T. N., Zaitsu, K., Madden, B., McCormick, D. J., and Toft, D. O. (1993) *Mol. Cell. Biol.* **13,** 869–876
3. Lassle, M., Blatch, G. L., Kundra, V., Takatori, T., and Zetter, B. R. (1997) *J. Biol. Chem.* **272,** 1876–1884
4. Blatch, G. L., Lassle, M., Zetter, B. R., and Kundra, V. (1997) *Gene* (*Amst.*) **194,** 277–282
5. Chen, S., Prapapanich, V., Rimerman, R. A., Honore, B., and Smith, D. F. (1996) *Mol. Endocrinol.* **10,** 682–693
6. Scheufler, C., Brinker, A., Bourenkov, G., Pegoraro, S., Moroder, L., Bartunik, H., Hartl, F. U., and Moarefi, I. (2000) *Cell* **101,** 199–210
7. Nicolet, C. M., and Craig, E. A. (1989) *Mol. Cell. Biol.* **9,** 3638–3646
8. Torres, J. H., Chatellard, P., and Stutz, E. (1995) *Plant Mol. Biol.* **27,** 1221–1226
9. Joshi, M., Dwyer, D. M., and Nakhasi, H. L. (1993) *Mol. Biochem. Parasitol.* **58,** 345–354
10. Irmer, H., and Hohfeld, J. (1997) *J. Biol. Chem.* **272,** 2230–2235
11. Ratajczak, T., and Carrello, A. (1996) *J. Biol. Chem.* **271,** 2961–2965
12. Webb, J. R., Kaufmann, D., Campos-Neto, A., and Reed, S. G. (1996) *J. Immunol.* **157,** 5034–5041
13. Duina, A. A., Marsh, J. A., and Gaber, R. F. (1996) *Yeast* **12,** 943–952
14. Lam, E., Martin, M., and Wiederrecht, G. (1995) *Gene* (*Amst.*) **160,** 297–302
15. Blecher, O., Erel, N., Callebaut, I., Aviezer, K., and Brieman, A. (1996) *Plant Mol. Biol.* **32,** 493–504
16. Radanyi, C., Chambraud, B., and Baulieu, E.-E. (1994) *Proc. Natl. Acad. Sci.* **91,** 11197–11201
17. Lamb, J. R., Tugendreich, S., and Hieter, P. (1995) *Trends Biochem. Sci.* **20,** 257–259
18. Blatch, G. L., and Lassle, M. (1999) *BioEssays* **21,** 932–939
19. Das, A. K., Cohen, P. T. W., and Barford, D. (1998) *EMBO J.* **17,** 1192–1199
20. Russell, L. C., Whitt, S. R., Chen, M.- S., and Chinkers, M. (1999) *J. Biol. Chem.* **274,** 20060–20063
21. Brinker, A., Scheufler, C., von Der Mulbe, F., Fleckenstein, B., Herrmann, C., Jung, G., Moarefi, I., and Hartl, F. U. (2002) *J. Biol. Chem.* **277,** 19265–19275
22. Sambrook, J., Fritsch, E. F., and Maniatis, T. (1989) *Molecular Cloning: A Laboratory Manual*, 2nd Ed., Vol. 1, pp. 7.46–7.50, Cold Spring Harbor Laboratory, Cold Spring Harbor, NY
23. Bradford, M. M. (1976) *Anal. Biochem.* **72,** 248–254
24. Laemmli, U. K. (1970) *Nature* **227,** 680–685
25. Towbin, H., Staehlin, T., and Gordon, J. (1979) *Proc. Natl. Acad. Sci. U. S. A.* **76,** 4350–4354
26. van der Spuy, J., Kana, B. D., Dirr, H. W., and Blatch, G. L. (2000) *Biochem. J.* **345,** 645–651
27. Wallace, L. A., Sluis-Cremer, N., and Dirr, H. W. (1998) *Biochemistry* **37,** 5320–5328
28. Liu, F.-H., Wu, S.-J., Hu, S.-M., Hsiao, C.-D., and Wang, C. (1999) *J. Biol. Chem.* **274,** 34425–34432
29. Ballinger, C. A., Connell, P., Wu, Y., Hu, Z., Thompson, L. J., Yin, L.-Y., and Patterson, C. (1999) *Mol. Cell. Biol.* **19,** 4535–4545
30. Hohfeld, J., Minami, Y., and Hartl, F. U. (1995) *Cell* **83,** 589–598
31. Smith, D. F. (1998) *Biol. Chem.* **379,** 283–288
32. Kraulis, P. (1991) *J. Appl. Crystallogr.* **24,** 946–950
33. Hernandez, M. P., Sullivan, W. P., and Toft, D. O. (2002) *J. Biol. Chem.* **277,** 38294–38304